

Oxygen Precipitate Studies in Silicon For  
Gettering in Solar Cell Applications

by

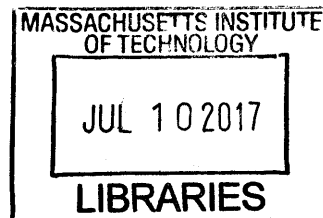
Ashley Salomon

SUBMITTED TO THE DEPARTMENT OF MATERIALS SCIENCE AND  
ENGINEERING IN PARTIAL FULFILLMENT OF  
THE REQUIREMENTS FOR THE DEGREE OF

BACHELOR OF SCIENCE IN MATERIALS SCIENCE AND ENGINEERING  
AT THE  
MASSACHUSETTS INSTITUTE OF TECHNOLOGY

JUNE 2001

Copyright 2001 Ashley Salomon. All rights reserved.



ARCHIVES

The author hereby grants MIT permission to reproduce and  
to distribute publicly paper and electronic copies of this thesis document  
in whole or in part

Signature redacted

Signature of Author:.....

.....  
Department of Materials Science and Engineering

May 17, 2001

Signature redacted

Certified:.....

.....  
Lionel C. Kimerling  
Prof. of Materials Science and Engineering & Director of Microphotonics Ctr

Thesis Supervisor

Signature redacted

Accepted by:.....

.....  
Ronald M. Latanision

Chairman, Undergraduate Thesis Committee

The author hereby grants to MIT permission to  
reproduce and to distribute publicly paper and  
electronic copies of this thesis document in  
whole or in part in any medium now known or  
hereafter created.

# Oxygen Precipitation Studies in Silicon for Gettering in Solar Cell Applications

By

Ashley Salomon

Submitted to the Department of Materials Science and Engineering  
On May 17<sup>th</sup>, 2001

## Abstract

Oxygen precipitates in silicon can be used (in a process called internal gettering) as sites of heterogeneous nucleation of precipitates of iron and other transition metal that are harmful to solar cell device operation. Oxygen precipitate densities in p- ( $10^{14}$  boron atoms/cm<sup>3</sup>) wafers were quantified using chemical etch techniques. The precipitate densities were then used to estimate times to getter iron based on a diffusion limited precipitation model. Oxygen precipitate densities in p++ ( $10^{19}$  boron atoms/cm<sup>3</sup>) wafers were quantified using chemical etch techniques. High levels of boron in p++ wafers make quantifying precipitate densities particularly difficult, via etching, or other methods because precipitate densities in highly doped wafers are very high and the size of precipitates small.

## **Acknowledgements**

I would like to give special thanks to Prof. Kimerling for his guidance and ideas. Prof. Kimerling gave me much freedom in my work and experimentation. I would like to thank Aimee Smith for her guidance, teachings and time spend in lab with me. Without Jurgen's help, I would not have been able to accomplish my goals, or obtain results from my experimentation. Jurgen spent many hours in lab with me helping me fix equipment and running the EBIC equipment.

# Table of Contents

<b>Title.....</b>	<b>1</b>
<b>Abstract.....</b>	<b>2</b>
<b>Acknowledgements.....</b>	<b>3</b>
<b>Table of Contents.....</b>	<b>4</b>
<b>List of Figures.....</b>	<b>5</b>
<b>1.0 Introduction.....</b>	<b>6</b>
<b>1.1 Statement Objectives.....</b>	<b>6</b>
<b>1.2 Background.....</b>	<b>7</b>
<b>1.2.1 Solar Cell Device Physics.....</b>	<b>7</b>
<b>1.2.2 Internal Gettering.....</b>	<b>11</b>
<b>1.2.3 Oxygen Precipitation.....</b>	<b>14</b>
<b>1.2.4 Schottky Contacts.....</b>	<b>15</b>
<b>1.3 Experimental Methods.....</b>	<b>16</b>
<b>1.3.1 Samples.....</b>	<b>16</b>
<b>1.3.2 Etch pit analysis p- silicon: Etching and EBIC.....</b>	<b>17</b>
<b>1.3.3 Etch pit analysis p++ silicon: Etching and OPP.....</b>	<b>19</b>
<b>1.4 Results and Discussion.....</b>	<b>21</b>
<b>1.4.1 p- Oxygen Precipitate Densities.....</b>	<b>21</b>
<b>1.4.2 Gettering Process Simulation in p- Samples.....</b>	<b>24</b>
<b>1.4.3 Schottky Contacts and EBIC.....</b>	<b>25</b>
<b>1.4.4 p++ Oxygen Precipitate Densities and OPP.....</b>	<b>26</b>
<b>1.5 Conclusions.....</b>	<b>28</b>
<b>1.6 Future Work: Gettering Experiments.....</b>	<b>28</b>
<b>1.7 Appendix.....</b>	<b>30</b>

**1.8 References.....31**

**List of Figures**

Figure 1 Silicon band-gap with Fermi level and electron-hole pairs.....9

Figure 2 Solar cell p-n junction.....9

Figure 3 I-V curve for solar cell during illumination and in darkness.....11

Figure 4 Curves of [Fe] vs. time for various densities of oxygen precipitates.....13

Figure 5 Photograph of etch pits of defects induced by oxygen precipitates in p- sample with 1hr LO anneal (750<sup>0</sup> Celsius) and 16hr HI anneal (1000<sup>0</sup> Celsius).....21

Figure 6 Photograph of etch pits of defects induced by oxygen precipitates in p- sample with 2hr LO anneal (750<sup>0</sup> Celsius) and 16hr HI anneal (1000<sup>0</sup> Celsius).....21

Figure 7 Photograph of etch pits of defects induced by oxygen precipitates in p- sample with 4hr LO anneal (750<sup>0</sup> Celsius) and 16hr HI anneal (1000<sup>0</sup> Celsius).....22

Figure 8 Comparison on oxygen precipitate densities in p- wafers to simulation models of oxygen precipitation at same temperature and time anneals.....23

Figure 9 I-V curve of titanium Schottky contact taken with measurement tools on DLTS machine to examine rectifying behavior.....25

Figure 10 [Fe] vs. Diffusion Length curves compiled from EBIC data on recombination lifetime of minority carriers.....26

Figure 11 Photograph of etch pits formed by oxygen precipitates in p++ wafer annealed at 650<sup>0</sup> Celsius for 7hrs and 1000<sup>0</sup> Celsius for 8 hrs.....27

Figure 12 Normal Coefficient vs. Temperature from DLTS.....30

Figure 13 1/C<sup>2</sup> vs. Voltage Plot from DLTS.....30

## **1.0 Introduction**

Solar cells and integrated circuits are dependent on defect control in silicon for high efficiency and performance. Contamination can be controlled by gettering at sites of lower chemical potential or faster precipitate rates for an impurity. Gettering is a relatively inexpensive method to lower transition metal content in electronic devices. Silicon device processing must be consistent with the gettering process to be effective.

As petroleum resources dwindle, the need for alternative energy resources increases. Improving solar cell efficiency will increase the utility of solar electricity. In order to make solar cells marketable, they must be both inexpensive and efficient. The silicon source material used in solar cell fabrication is most often the least expensive and most contaminated stock available. Thus, commercial solar cells are less efficient though less expensive. Optimal processing could upgrade the performance of the cheaper silicon, to high efficiency. These techniques for improving solar cell efficiency must be cost effective. This study addresses defect control techniques that are carried out with simple and inexpensive heat treatments.

### **1.1 Statement of Objectives**

Transition metals can be easily and unintentionally incorporated into silicon because they are prevalent, fast diffusers and relatively soluble in silicon at processing temperatures. Once in silicon, they form deep electronic levels that act as recombination centers, reducing minority carrier lifetime. The presence of these metals reduces efficiency in solar cell pn-junction diodes by attenuating the junction photo current. In order to remedy this problem, it is important to understand potential gettering mechanisms.

Oxygen precipitates in bulk silicon act as sites for the heterogeneous nucleation of transition metal contaminant precipitates. Precipitation effectively removes the transition metal impurities from electrical activity. To determine how oxygen precipitation affects gettering in silicon for photovoltaic applications, precipitate densities must be quantified (see equation (10)). Once precipitate densities have been quantified, times to getter transition metals can be estimated with a diffusion-limited precipitation model and gettering experiments be designed. In the gettering experiments, various concentrations of contaminants are diffused into silicon wafers with varying concentrations of oxygen precipitates. In this study, precipitate formation in p-type silicon is standard because solar cells and integrated circuits are constructed on p-silicon substrates. The design is based on the high mobility of the minority carrier electrons. Gettering is an important contamination prevention strategy for lost cost fabrication of high performance components.

## **1.2 Background**

### **1.2.1 Solar Cell Device Physics**

A solar cell is a p-n junction diode that produces electron and hole currents from photon absorption. Silicon for solar cell applications is often p-doped, meaning that a Group III element from the periodic table such as boron is introduced into the silicon lattice. These atoms do not have enough valence electrons to satisfy four covalent bonds with the surrounding silicon atoms, giving rise to the lack of an electron (a hole) tied to the Group III atom. If the silicon is doped with a Group V atom from the periodic table, four of the electrons will form a covalent bond with the surrounding silicon atoms, but one electron will remain in excess giving rise to an extra electron carrier. This type of

doped silicon is called n-type. The energy required to release the hole from p-type silicon is [1]:

$$E = \frac{m_{eff} * q^4}{8\epsilon_0^2 h^2} = .02eV \quad (1)$$

Where  $m_{ef}$  is the effective mass of the hole,  $q$  is the charge of the hole,  $\epsilon_0$  is the permittivity of free space, and  $h$  is Planck's constant. This required energy is less than that of silicon's 1.1 eV band-gap because the charge carrier is partially freed from the boron atom. This ionization energy is basically the ionization energy of the hydrogen atom that is reduced by the dielectric screening term,  $\epsilon_0^2$ . Electron and hole carriers, once excited to the conduction, or valence band are mobile in two ways: drift and diffusion. Under an applied electric field, the holes or electrons move with a certain velocity. In a crystalline lattice, the particles will collide with other atoms in the lattice. The current density flow due to drift for holes is [1]:  $J_h = q\mu_h pE$

(2)

Where  $q$  is hole charge,  $\mu_h$  is the hole mobility,  $p$  is the hole concentration, and  $E$  is the electric field. This holds true for current density flow of electrons if hole mobility is replaced with electron mobility and  $p$  is replaced with electron concentration,  $n$ . Carriers can also flow by diffusion[1]:

$$J_h = -qD_h \frac{dp}{dx} \quad (3)$$

$$J_e = qD_e \frac{dn}{dx} \quad (4)$$

Where  $q$ ,  $p$  and  $n$  are as above, and  $D$ 's are the diffusion constants for  $e$ 's and  $h$ 's respectively. The sign difference is due to the opposite polarity of charges involved.



Current is proportional to the flux of charged particles so current density can be treated as a one-dimensional concentration gradient.

A large number of occupied states are present in the valence band separated by largely unoccupied states in the conduction band. Absorption is likely when the energy of photons making up the light is larger than the forbidden band gap[1]. A photon excites electrons from the valence to the conduction band leaving behind a hole, thus generating an electron-hole pair. Electron-hole pairs fall back to their original states by a process called recombination. The primary process that affects solar cells is called trap recombination. Impurities and defects in semiconductors can give rise to energy levels within the “forbidden” gap of silicon. Electrons can relax back into these impurity energy levels, and then relax back into the valence band annihilating a hole:

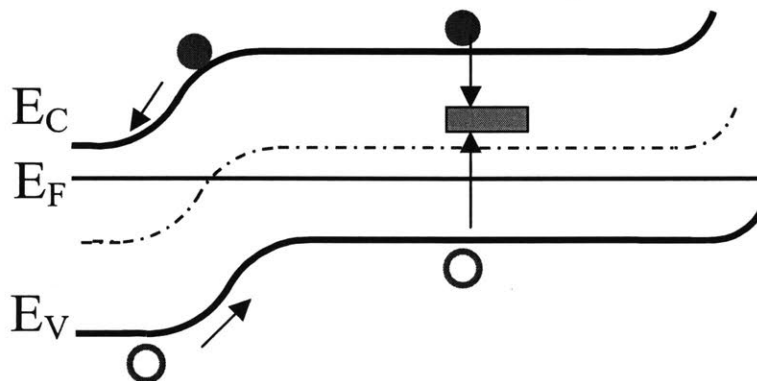


*Figure 1: Electron-Hole Recombination at Electronic Sites within Silicon’s Band-Gap*

The most common type of solar cells are made by forming a junction between p-type and n-type silicon:

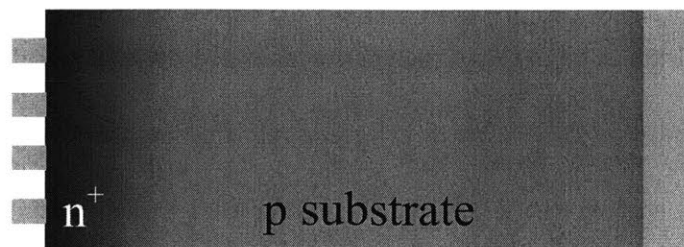


*Figure 2: Common Solar Cell Device Layout*

Electrons flow easily through the n-type region due to their majority carrier status, while holes flow easily through the p-type region due to the high density of holes. When the n and p regions are brought together, the higher concentration of electrons in the n type region will flow to the p type region leaving behind positively charged ionized donors. Similarly, holes leaving the p region will expose negatively charged ionized donors. The charged regions will form an electric field that will oppose the natural diffusion and equilibrium will be reached. This region is called the depletion region and is present at the junction between p and n.

When light enters a solar cell, the electron-hole pair is created. The minority carriers in the larger p-region of the diode (the electrons) must cross the depletion region by diffusion in order to produce current. The p-region of the device is often large in order to take advantage of the larger mobility of electrons as minority carriers (electrons). The larger the diffusion length ( $L_D$ ) to the junction, the greater the number of minority carriers that can diffuse to the junction. The current produced when the solar cell is illuminated is directly dependent on  $L_D$  [2]:

$$I_{sc} = qAG(W + L_D) \quad (5)$$

Where  $q$  is the charge of one electron,  $A$  is the cross-sectional area of the diode,  $W$  is the width of the depletion region, and  $G$  is a factor of illumination (in the dark  $G = 0$ ). The open circuit voltage (voltage when device is illuminated and no load is present) is proportional to the natural log of the current during illumination [2]:

$$V_{oc} = \frac{kT}{q} \ln\left(\frac{I_{sc}}{I_o} + 1\right) \quad (6)$$

Where  $T$  is temperature,  $k$  is Boltzman's constant, and  $I_o$  is the leakage current when the device is not illuminated. The leakage current is dependant on the concentration of holes

and electrons from doping, the diffusion lengths of the holes and electrons, and the diffusion constants of the holes and electrons.

When the solar cell is illuminated, the current versus voltage curve looks as follows:

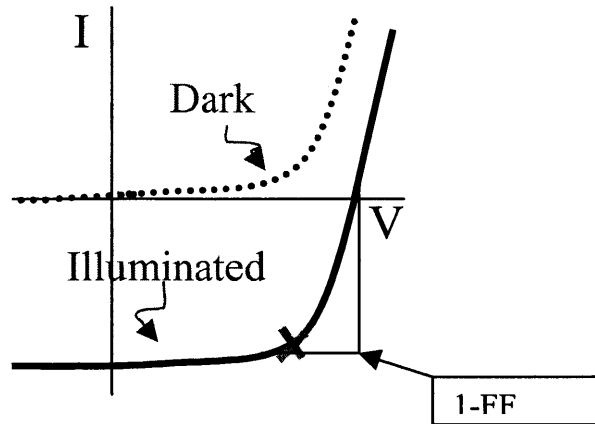


(Figure 3): *I-V Curve for Solar Cell Device Output with and without Illumination*

FF (fill factor) is the ratio of current  $I$  to voltage  $V$  when the device is illuminated. It is affected by device design. For example, a solar cell might have large contacts, forfeiting a larger surface area for light to enter the device. The device factors previously mentioned play a role in the efficiency  $\eta$  of a solar cell [2]:

$$\eta = \frac{FF * I_{sc} V_{oc}}{P_{IN}} \quad (7)$$

Where  $P$  is the total power into the device from sunlight. From this equation, one can see that the efficiency is directly effected by  $L_D$ .

### 1.2.2 Internal Gettering

As previously mentioned in 1.1.2, recombination centers formed by defects and impurities in silicon can cause electron-hole pair recombination. As an example, Fe in the silicon matrix has an electronic state within the band gap of silicon that will enhance the recombination rate, and decrease the number of minority carrier electrons that will

survive long enough to cross the junction. The time constant for exponential decay of excess carrier recombination is called the minority carrier lifetime,  $\tau_e$ . The minority carrier lifetime is related to the minority carrier diffusion length by [2]:

$$\tau_e = L_e^2 D_e \quad (8)$$

Where  $D_e$  is the diffusion constant for the electron, and  $L_e$  is the diffusion length for an electron. Many mechanisms for minority carrier recombination exist that will shorten  $\tau_e$ .  $\tau_e$  for Fe deep levels is [3]:

$$\tau_e = \tau_{Fe} = \frac{1}{\sigma_n v_{th} [Fe]} \quad (9)$$

Where  $[Fe]$  is the concentration of iron in the silicon,  $v$  is the thermal velocity, and  $\sigma$  is the capture cross-section for iron.  $\sigma_n \approx 10^{14} \text{ cm}^{-2}$  and  $v_{th} \approx 10^7 \text{ cm/s}$ . An increase in iron decreases the minority carrier lifetime. As a result, diffusion length decreases, decreasing efficiency in the solar cell.

Gettering is a general term for the removal of iron and other transition metals. In order to determine the optimal process for fabricating silicon wafers (to getter transition metals more effectively) an understanding of oxygen precipitation in silicon and how it internally getters iron in silicon is desired. The precipitates act as heterogeneous nucleation sites for the precipitation of  $[Fe]$  in solution [4]. The charge of  $[Fe]$  with respect to time obeys diffusion limited kinetics according to an equation involving the density of internal oxygen precipitate gettering sites [3]:

$$\frac{\partial C}{\partial t} = D_{Fe} \frac{\partial^2 C}{\partial^2 X} + 4\pi r N_{IG} D_{Fe} (C_{sol} - C(t)) \quad (10)$$

Where  $C_{sol}$  is Fe solubility in silicon, and  $C(t)$  is change in concentration over time. The first part of this equation is a Fick's Law relation, while the second term of the equation arises from oxygen precipitates that serve as heterogeneous nucleation sites for super-saturated Fe. As the silicon is cooled from processing temperatures [4]:

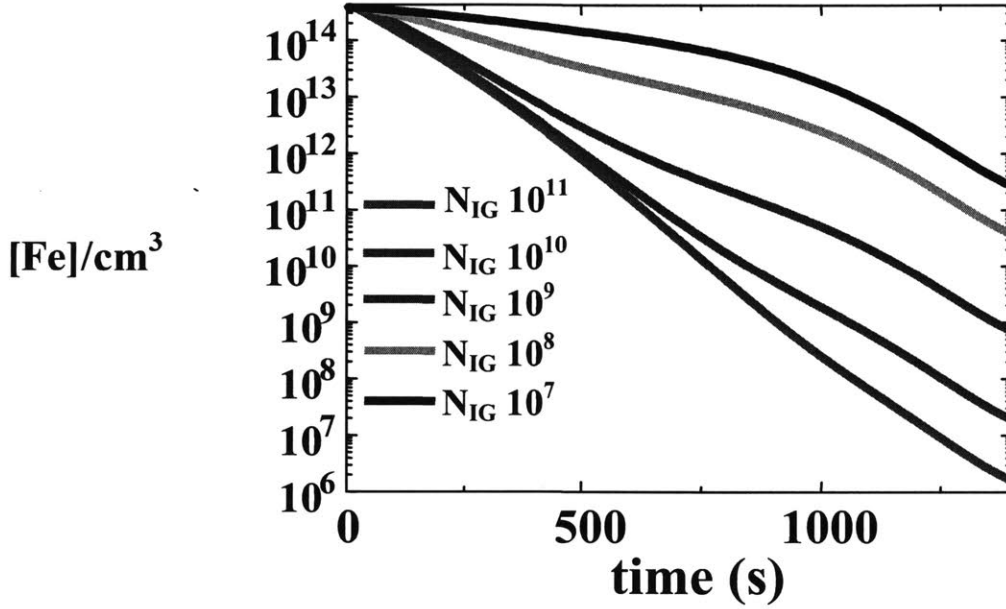


Figure 4:  $[Fe]$  vs. Cooling time ( $1^\circ$  Celsius degree per second) in silicon at different densities of oxygen precipitates ( $N_{IG}$ ).

the  $[Fe]$  becomes supersaturated. The driving force for precipitation is then  $C_{sol} - C(t)$ .

From equation (10), one can see that two possible diffusion-limited gettering mechanisms exist for iron: outdiffusion towards the silicon surface from Fick's law and diffusion-limited heterogeneous precipitate formation [3]:

$$\tau_{outdiffusion} \propto \frac{(t_{Si} / 2)^2}{D_{Fe}} \quad (11)$$

$$\tau_{IG} = \frac{1}{4\pi r N_{IG} D_{Fe}} \quad (12)$$

Where  $t_{Si}$  is the silicon thickness,  $r$  is the average size of precipitate radii, and  $\tau$  is the time for outdiffusion (11), or the time for capture at precipitate sites (12). Clearly outdiffusion of Fe away from the silicon is most desired, but oxygen precipitates, which

will be formed in the silicon as an outcome of wafer processing, can be optimized for Fe gettering mechanisms (see section 1.4.2 for measurements). Depending on the iron contamination level, one of the terms in (10) will dominate. To predict internal gettering by precipitates,  $N_{IG}$ , the precipitate density, must be known.

Oxygen precipitates provide heterogeneous nucleation sites that serve to aggregate dissolved Fe contaminants by two mechanisms: capture at the  $\text{SiO}_2 / \text{Si}$  interface, or capture in dislocation loops introduced by the precipitates. Oxygen precipitates serve to lower the barrier to nucleation.

### 1.2.3 Oxygen Precipitation

In C-Z grown silicon there is an inherent amount of interstitial oxygen. During the process of wafer fabrication, wafers are annealed and cooled, inducing the formation of oxygen precipitates from interstitial oxygen [5]. During device processing, or a preannealing treatment, outdiffusion of oxygen at the surface can be prominent enough that the supersaturation at the surface (within a depth of ~3-10 microns) decreases and  $\text{SiO}_2$  precipitates cannot form until that depth [5]. This precipitate free depth is called the denuded zone. The denuded zone is an important parameter in device processing because precipitates are harmful in certain regions of the device.

Oxygen precipitate formation for the purposes of internal gettering can be modeled by homogeneous nucleation [6]. In this model, the rate of oxygen precipitate nucleation  $J$ , is proportional to  $C_{cri} \propto C_i e^{-\frac{1}{T}}$  where  $C_{cri}$  is the critical nucleus density,  $C_i$  is the interstitial oxygen concentration present in the silicon lattice and  $T$  is temperature [7]. Although the rate of nucleation appears linearly dependent, it eventually reaches an asymptotic value as the oxygen is precipitated and outdiffused from the silicon. The

growth step of precipitate formation, once the precipitate have nucleated, is modeled by an oxygen diffusion-limited growth model [8]. For the growth time  $t$ , the radius size  $r$  of the precipitates follows the model:

$$r = [\Omega_{ox} D_i (C_i - C_i^{eq}) t]^{\frac{1}{2}} \quad (13)$$

Where  $D$  is the diffusion constant for oxygen,  $C_i$  is the equilibrium oxygen concentration, and  $C_i^{eq}$  is the thermal equilibrium oxygen concentration. Precipitates grown in silicon wafers for the purposes of studying bulk precipitation are often grown with a LO-HI anneal treatment. The first anneal is often for a period of under ten hours, and the temperatures do not exceed 700 Celsius. This lower temperature step produces nucleation.  $J$  is inversely proportional to the exponential of temperature, so if the temperature is too high the rate of nucleation will be too low. The HI step, a longer anneal at temperatures of around 1000° Celsius, causes growth of the already nucleated precipitates. There is an increasing influence of thermal history on the calculated precipitate density the shorter the duration of the LO anneal at temperatures around 700 Celsius [6].

HI-LO-HI treatments are used to produce high levels of outdiffusion of oxygen, producing a denuded zone. The occurrence of the denuded zone is influenced by outdiffusion during the first anneal, for which a higher temperature is chosen than in succeeding anneals [9]. Oxygen precipitates, with these treatments, steadily increase from zero concentration around a depth of microns, until a constant bulk concentration is reached. Denuded zone depths increase with higher annealing temperature and duration, but decrease with increasing initial oxygen concentration [10].

## 1.2.4 Schottky Contacts

Successful Schottky contacts depend on the interface between metal and silicon, and the built-in voltage. The built-in voltage is theoretically defined as the difference between the metal work function  $\Phi_M$ , and the electron (or hole) affinity of the silicon [3]. Once a Schottky junction has been formed by evaporating metal (titanium for p-type silicon and gold for n-type silicon) holes for p-type devices (such as solar cells used in this application) diffuse to the metal side leaving a negative space charge region. Eventually these holes are stopped by an opposing electric field created by the negative acceptor charge left behind as in the p-n junction case [3].

## 1.3 Experimental Methods

### 1.3.1 Samples

Silicon wafers from Komatsu Japan were obtained for purposes of quantifying oxygen precipitate density. One set of wafers, containing a p++ ( $10^{19}$  boron atoms/cm<sup>3</sup>) bulk with a p epitaxial surface was annealed in industry at 650<sup>0</sup> Celsius for LO treatment and at 1000<sup>0</sup> Celsius for a 16 hour HI treatment. These samples, once the oxygen precipitate density was quantified, were to be used in iron gettering experiments. Because p++ wafers have a high, difficult to control chemical etch rate, p- wafers were first etched to reveal defects formed from precipitates. Unlike p++ wafers, p- wafers were not industrially annealed, and contained  $1 \times 10^{17}$  atoms/cm<sup>3</sup> interstitial oxygen concentration. P- wafers with an initial oxygen concentration of  $10^{14}$  boron atoms/cm<sup>3</sup> were annealed in a horizontal furnace at 750<sup>0</sup> Celsius for 1, 2 and 4 hours LO treatments, and all Hi treatments were carried out at 1050<sup>0</sup> Celsius for 16 hours. These temperatures were chosen to give a range of precipitate density variation to compare with simulations



carried out on wafers with the same initial oxygen concentration and precipitate annealing times.

### **1.3.2 p- Chemical Etching and EBIC**

Optimal etching procedures for p- wafers were determined. p- wafers were solvent cleaned with trichloroethane, acetone and methanol, respectively, for five minutes in each solvent. A 4:1:1 HNO<sub>3</sub>:HAc :HF (Nitric Acid: Acetic Acid: Hydrofluoric Acid) isotropic polishing etch was then used for 50 seconds to smooth the surface. More isotropic etches such as 1:15:3:3 HF:HNO<sub>3</sub>:HAc:H<sub>2</sub>O and HF:HNO<sub>3</sub>:HAc 1:5:12 were found to produce defects that were difficult to decipher between. The MEMC chromate alternative etch, HF:HNO<sub>3</sub>:HAc:H<sub>2</sub>O (36:25:18:21) with 1 gram Cu(NO<sub>3</sub>)<sub>2</sub>·3H<sub>2</sub>O per 100 mL of mixed acid was used to reveal etch pits and stacking faults formed from oxygen precipitation. Black wax was melted on the backside of each samples in order to prevent etching through the backside poly. Sample pieces were etched at 15, 30, 45 and 60 seconds. Once etched, a profilometer was used to measure etch depth of each sample. Photographs with a 35mm camera connected to a Zeiss optical microscope were taken of each sample in multiple locations. Precipitates were counted over 20 x 20 micron areas 30 times and averaged. Depths found from profilometer readings were used to find densities of each of the 15, 30, 45, and 60 second etches. If silicon is etched too deeply, the history of etching is lost. Because a three dimensional etch number is desired, it is necessary to ensure that both old and new precipitates are seen. Eventually, when etched far enough, the same number of old and new precipitates are lost and gained, respectively, and a steady states number will be reached. This is not desired because the three dimensional profile can no longer be counted. Precipitate densities were compared

at the four different etch times to ensure that etch pit counting was in the linear region of density versus depth, such that density doubled as depth doubled and the history of all etch pits could be seen. All etch times were found to be within the linear range for counting precipitates. Precipitate densities were then compared with simulations of silicon annealed with the same LO-HI treatment from Schrems et al [11].

Scanning Electron Microscope Electron Beam Induced Current (SEM-EBIC) can be used to count oxygen precipitates and compare with chemical etch method. Using SEM equipment in conjunction with measuring I-V characteristics of diffused p-n junctions in the presence of oxygen precipitate defects, electrical activity can be determined. Unetched 1, 2 and 4 hour LO anneal (all with 16h HI anneal) were taken from the same batch as the etched samples, solvent cleaned in same manner as for chemical etching, chemically polished with 4:1:1 acid mixture, and then placed in 100:1 HF: DI WATER solution to remove oxide. Samples were immediately mounted in an evaporator system and the evaporator chamber was evacuated to  $7.5 * 10^{-7}$  millibar to prepare for evaporation of Schottky contacts. Titanium metal must be used on p-type silicon in order to produce a rectifying contact. Titanium was weighed with a microgram balance and measured by the following equation to produce 1000 angstrom thickness contacts:

$$d = \frac{M_e h^2}{\pi \rho r^4} \quad (14)$$

Where d is the thickness of the evaporated contacts,  $M_e$  is the mass of the metal, h is the height of the evaporative chamber, p is the density of the metal, and r is the radius of the evaporative chamber. This equation assumes evaporation of metal  $360^{\circ}$  around the

source. Thus this thickness represents the thickness that will coat the entire inside of the evaporator dome, including the sample. A molybdenum shield with one millimeter thick holes was used to produce the circular contacts on the surface of the silicon samples. The shield must be laid evenly over the silicon, or metal will coat the surface area underneath the shield.

Once contacts were evaporated, liquid InGa was used as a back ohmic contact. The silicon was scratched with a diamond scribe 100 times to rid the back surface of the native oxide, then InGa was applied, and finally silver paint to secure the sample on the sample holder cleaned with methanol. The oxygen precipitates are electrically active, and can be seen in an EBIC image underneath a Schottky contact where current is induced. EBIC can also be used to measure minority carrier lifetimes, and thus diffusion lengths. Samples with varying amount of [Fe] and oxygen precipitate densities can be measured for minority carrier lifetimes and compared to reveal effectiveness of precipitate gettering.

To test the rectifying behavior of the contacts, I-V (current vs. voltage) curves were produced by a computer measurement program that measures changes in current in response to varying voltage through the silicon sample. This set-up is one test that can be run from the DLTS (Deep Level Transient Spectroscopy) equipment. Good Schottky contacts are not only desirable for EBIC, but are imperative for DLTS measurements of transition metals concentrations (see Appendix 1) if silicon samples with oxygen precipitates are to be contaminated in order to study gettering effects of precipitates.

### **1.3.3 p<sup>++</sup> Chemical Etching and OPP**

In order to etch the p<sup>++</sup> wafers, epitaxial layer and denuded zone were removed by

mechanically polishing. Samples were attached with black wax to a metal weight and polished at  $30\ \mu\text{m}$  for 2 hours,  $15\ \mu\text{m}$  for 30 minutes,  $5\ \mu\text{m}$  for 30 minutes,  $1\ \mu\text{m}$  for 30 minutes, and  $.3\ \mu\text{m}$  (with DI water so as not to scratch the surface) for 30 minutes.

Samples were observed under an optical microscope to ensure smoothness of surface and few scratches. Samples were polished down a total of  $40\ \mu\text{m}$ . After mechanical polish,

samples were solvent cleaned with trichloroethane, acetone and methanol, respectively, and polished with  $\text{HNO}_3:\text{HF}:\text{HAc}$  (4:1:1) isotropic etch for thirty seconds, and possibly longer if scratches were still present when observed under an optical microscope. A Piranha etch of  $\text{H}_2\text{SO}_4 : \text{H}_2\text{O}_2$  (3:1) was used for 10 minutes to remove any metals that might have contaminated the samples during mechanical polish. The MEMC etch for p- samples was too strong for the p++ samples, most likely because atoms in the lattice of more heavily doped wafers form higher energy bonds. Ultimately, a 1:15:3:3 ( $\text{HF} : \text{HNO}_3 : \text{CH}_3\text{COOH} : \text{H}_2\text{O}$ ) etch was used to reveal dislocation loops and etch pits at 15, 30 and 45 second etchings. As with the p- samples, a profilometer was used to measure etch depth. Defects were counted in thirty  $20 \times 20$  micron areas and densities of all three etch times were compared to ensure none of the sample were over-etched. Wafers from the same batch were sent to Accent Labs in California for OPP (Optical Precipitate Profiler) measurements of the p++ precipitate density because EBIC resolution is not high enough for deciphering between single precipitates. The OPP can image defects in surface and near-surface regions with a defect sensitivity of  $\sim 10$  nanometers. The OPP uses optical interference contrasting to detect defects. A laser is operated in the 1.3-micron range at the minimum of the adsorption curve for defects in silicon such that defects can be detected in heavily doped wafers.

## 1.4 Results and Discussion

### 1.4.1 p- Oxygen Precipitate Densities

I used 35mm film and a camera mounted on an optical microscope to image the

*Figure 5: 1hr LO annealed sample (750°C) with 16hr HI anneal and 30 sec MEMC etch:*

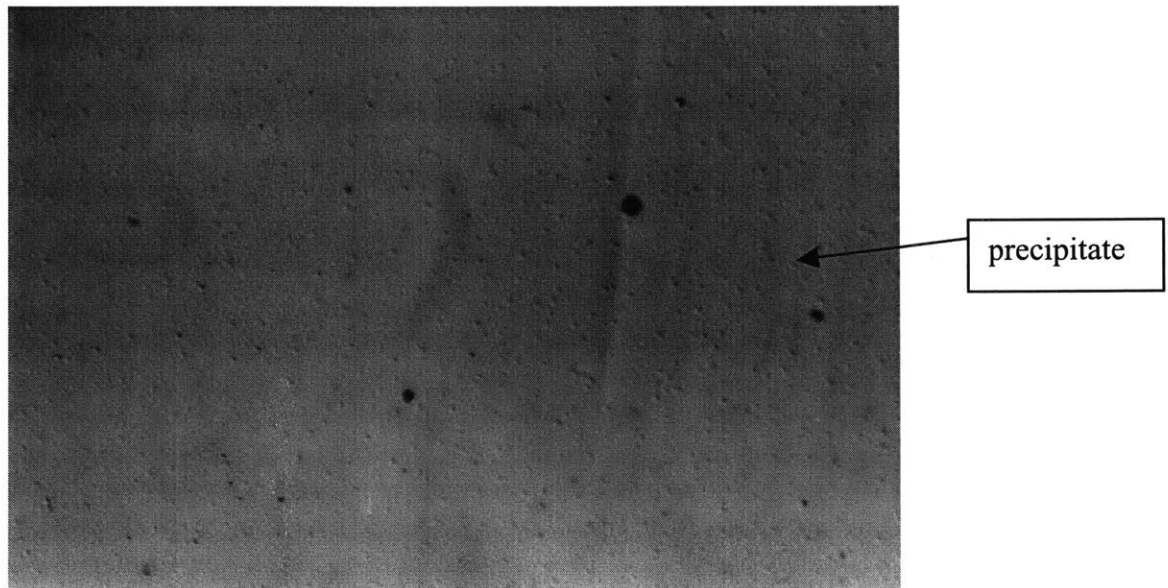


*Figure 6: 2hr LO step annealed sample (750°C) with 16hr HI anneal and 40 sec MEMC etch:*

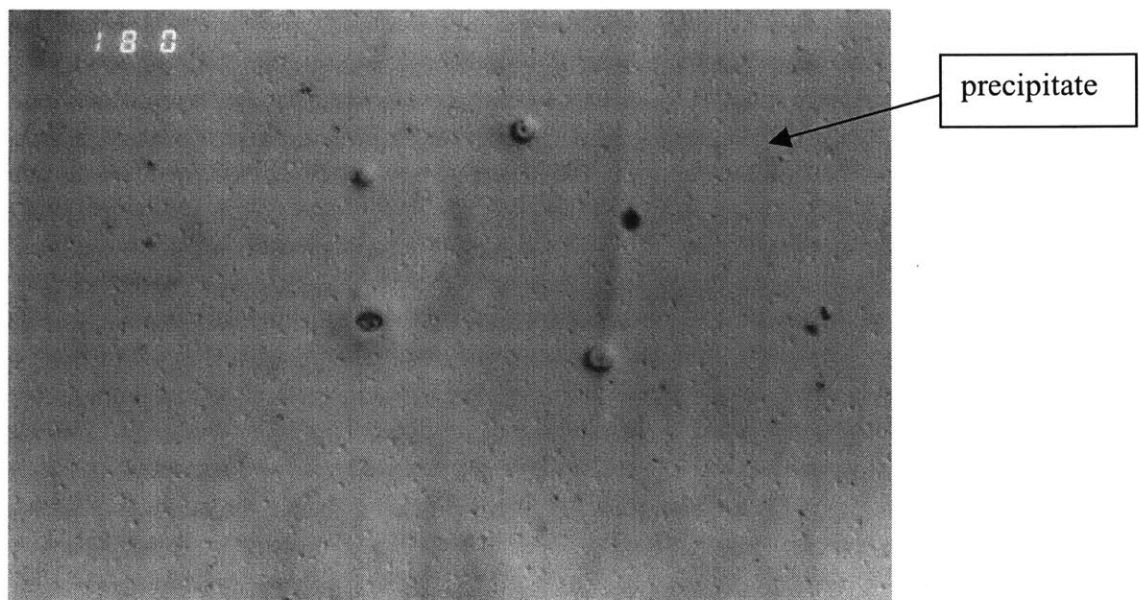
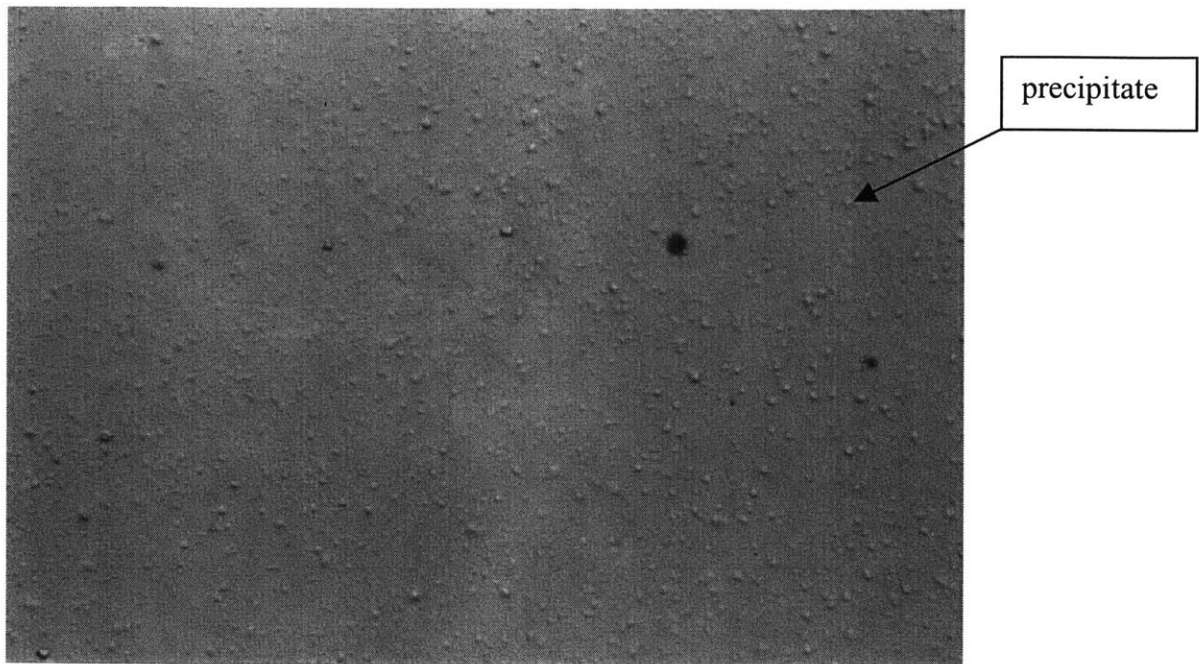


Figure 7: 4h LO-step annealed sample (750°C) with 16hr HI step and 30 sec MEMC etch:



7 photographs were taken of each etch at various times. A one minute etch time was found to be too long an etch time for the p- samples. Etch times of 40 seconds and less were found to be reasonable for counting precipitates accurately. Precipitates were counted in areas of 400 square microns, and profilometer measured etch depth to calculate an etch time of .67 microns/minute. From this information volume (and thus density) of space in which precipitates were counted was determined. Nineteen areas of 20 x 20 microns were chosen for counting precipitates, and averaged to find density per  $\text{cm}^3$ . For 1hr nucleation time (750 Celsius, 16h growth time) precipitate density was determined to be  $1.4 \times 10^{10} \text{ prec/cm}^3 \pm 0.38 \times 10^{10} \text{ prec/cm}^3$ . Although the standard deviation is large, a density in the range of the precipitate number is adequate for use in gettering experiments. For 2hr nucleation (750 Celsius, 16h growth time) precipitate density was determined to be  $3.64 \times 10^{10} \text{ prec/cm}^3 \pm 0.68 \times 10^{10} \text{ prec/cm}^3$ . For 4hr

nucleation (750 Celsius, 16h growth time) precipitate density was determined to be  $4.5 \times 10^{10} \text{ prec/cm}^3 \pm 0.36 \times 10^{10} \text{ prec/cm}^3$ .

In order to determine the accuracy of these numbers, data was compared to simulations of p wafers with the same annealing time, temperature and initial oxygen concentration made by Schrems et al [11]. Initial conditions were  $10^{14} \text{ atoms/cm}^3$  boron doped for p- wafers, while wafers in simulation were doped  $10^{16} \text{ atoms/cm}^3$ . Precipitate density from the p- wafers was thus expected to be lower from a lower boron concentration. The simulation was based on multiple equations defining precipitate formation a precipitate size distribution function dependent on precipitate radius and simulation time. This function varied with time.  $\text{SiO}_2$  precipitates were assumed, and an unstrained molecular  $\text{SiO}_2$  volume of  $v=4.5 \times 10^{-23} \text{ cm}^3$  was assumed. Gibb's free energy, oxygen diffusivity, solid solubility of oxygen, interfacial energy of the oxygen precipitates in the silicon matrix, and interstitial oxygen concentration were all taken into account in the simulation. The following figure compares experimental data to the simulation curve:

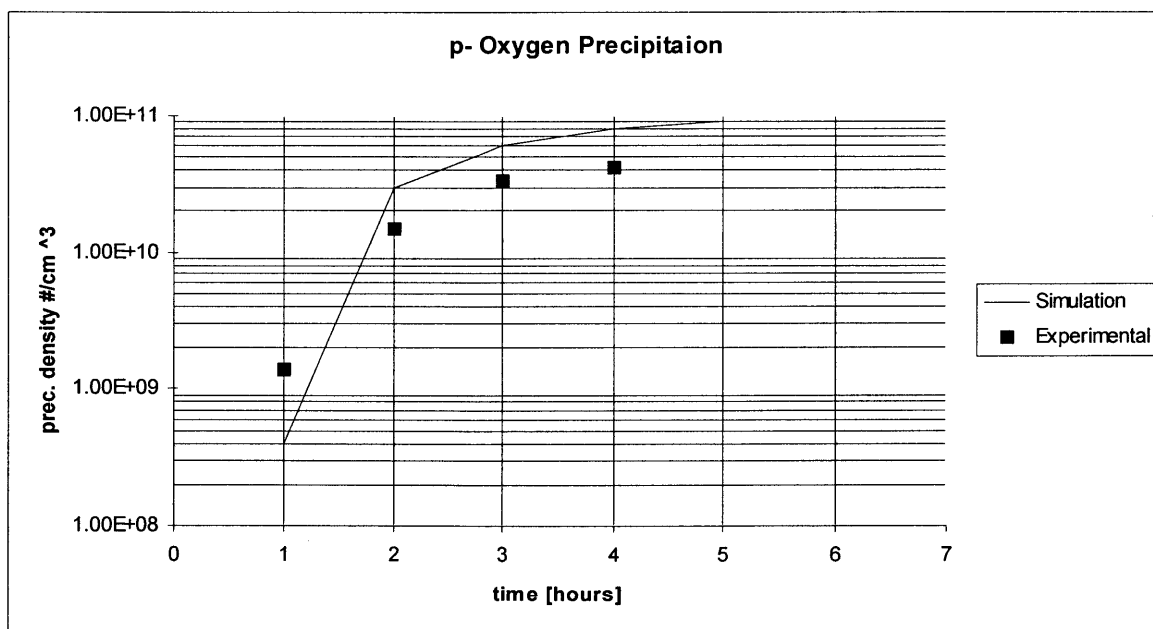


Figure 8: Experimental Oxygen Precipitate Densities compared Simulation curve of Oxygen Precipitate Densities at Same annealing times and temperature

The experimental data does follow the same trend as the simulation, however the observed precipitate density is slightly smaller. At higher doping levels there are effects from boron dopant concentration on oxygen precipitation. Interstitial boron allows for the accommodation of strain in the silicon lattice because boron atoms are smaller than silicon atoms. The straining effect increases solubility of silicon self-interstitials producing smaller sized, but larger amounts of precipitates and a fermi-level effect is believed to drive small aggregation reactions forward.

### 1.4.2 Gettering Process Design

Using precipitate densities found from p- etching of 4, 2, and 1hr LO anneals (750° Celsius) with 16hr HI anneal (1000° Celsius) and size estimates of precipitate radii at the 4hr, 2hr and 1hr LO anneal (750° Celsius) from simulations [11],  $\tau_{outdiffusion}$  and  $\tau_{IG}$  (equations (11) and (12)) values were estimated. Size radii were 7nm, .4nm, and .4nm for 4, 2, and 1hr LO anneal times, respectively. The silicon sample thickness is 100 microns. Fe diffusivity plotted against temperature graphs were used to determine  $D_{Fe} = 5e-7 \text{ cm}^2/\text{s}$  at 750° Celsius [3]. The following represent times in equation (10) and (11):

LO(750 C)	N(IG)/cm <sup>3</sup>	Time to Outdiffuse (11)	Time to Getter Internally (12)
1 hr	1.4*10 <sup>10</sup>	20sec	5.3min
2 hr	3.6*10 <sup>10</sup>	20sec	2.65min
4 hr	4.5*10 <sup>10</sup>	20sec	49sec

*Table 1:  $\tau_{outdiffusion}$  and  $\tau_{IG}$  times based on Oxygen Precipitate Densities found from p- Chemical Etching*

In this scenario, time for outdiffusion of iron from the silicon samples dominates, as more iron leaves the silicon sample than remains in the bulk region.



### 1.4.3 Schottky Contacts and EBIC

Using titanium for contacts, the following rectifying I-V curve was obtained:

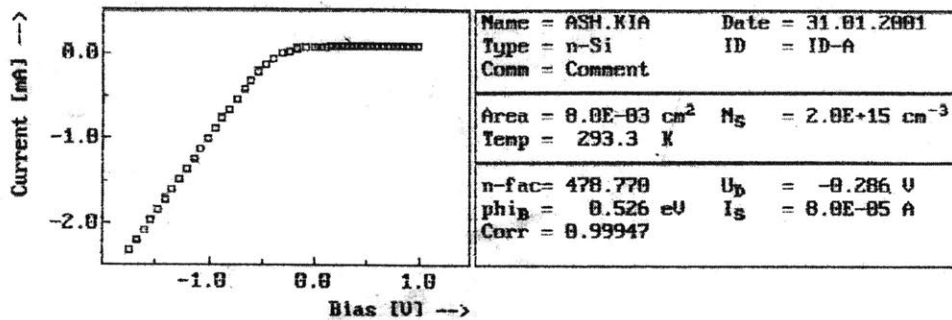
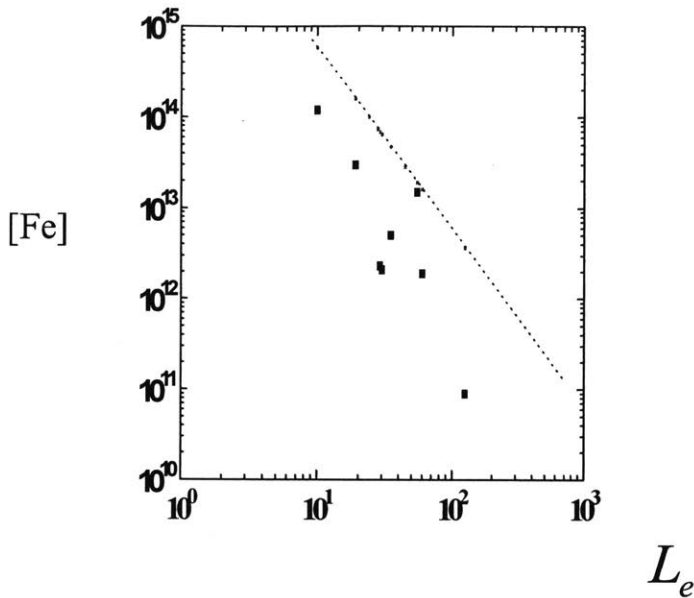


Figure 9: I-V Curve of a titanium contact on p-silicon

Although Schottky and Ohmic contacts were adequate, EBIC did not display a clear image for the 4hr and 2hr annealed samples. The image revealed was grayish in nature, without definite black and lighter zones. This occurrence is due the lack of resolution and contrast at such a high density of precipitates. The entire surface of the 1hr annealed sampled lit up on the screen at high electron beam intensity, revealing no distinction between contacts and surrounding surface. This suggests that a thin layer of titanium metal was present across the surfuace, creating one large contact. Metal can reach the area around the contact holes of the molybdenum shield. If the contact area is too large, the depletion region increases, and fewer carriers are collected making electrical detection more difficult. No space charge region is seen, and no contrast between electrically active precipitates and non-electrically active regions will be seen.

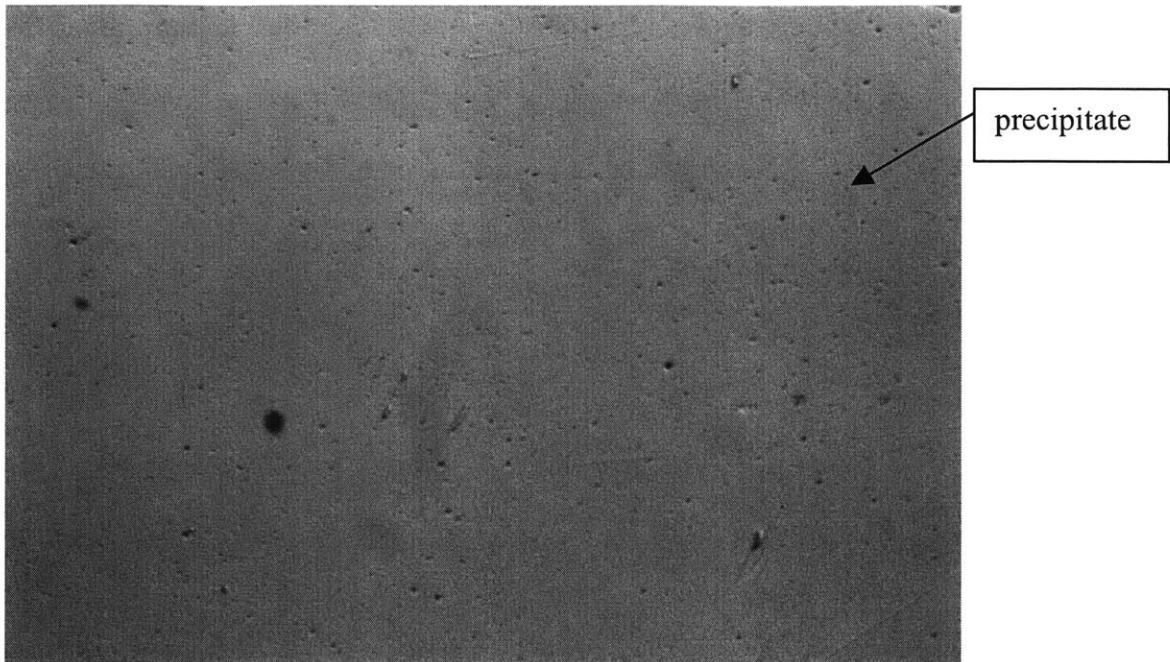
Past data for measurements of minority carrier recombination lifetime with EBIC in order to find diffusion length  $L_e$  (refer to equation (8)) reveal that as [Fe] decreases, diffusion length, and thus lifetime, increases [3]:

Figure 10: Diffusion Lengths with EBIC



#### 1.4.4 p++ Precipitate Density

From the chemical etching procedure,  $N_{IG}$  for p++ wafers was found to be  $7.5 \times 10^{10}$  prec/cm<sup>3</sup>  $\pm$   $0.41 \times 10^{10}$  prec/cm<sup>3</sup>. P++ samples are expected to have a much higher precipitate concentration than p wafers. Precipitates for these samples were nucleated at 650<sup>0</sup> Celsius, as opposed to 750<sup>0</sup> Celsius for the samples in 1.4.1. It is possible that this difference in temperature was a greater factor in the precipitate nucleation than the doping of the wafer, because the p++ samples do not fit the simulation model well. One would expect the density to be larger than for the p++ doped silicon, but this is not the case when compared with the precipitation simulator at the same anneal time:



*Figure 11: p++ silicon microimage of oxygen precipitates at 30 etch time*

OPP measurements were found to be inadequate (densities on the order of  $10^4$  prec/cm<sup>3</sup>). These measurements are much less than the expected value for highly doped wafers (on the order of  $10^{11}$  prec/cm<sup>3</sup>) [11]. In highly doped p++ wafers, precipitates formed are, on average, smaller than for more lightly doped wafers and the density is much greater. Resolution for OPP depends on the size of the laser beam used, which was on the order of a micron. This resolution was apparently inadequate to measure such small precipitates that were smaller than one micron. Photons from the laser beam will scatter off the precipitate surfaces, unless the laser range is too large. In this manner, precipitates smaller than one micron were not detected, and many small precipitates clumped together were likely confused for a single precipitate. Other OPP machines exist with much higher resolution that will be effective to count precipitate densities.

## 1.5 Conclusions

Oxygen precipitate density increases with increasing LO annealing time at 750° Celsius for p- silicon.  $N_{IG}$  densities using chemical etching techniques for p- silicon agree with simulation data. Predicted  $\tau$  (times to getter iron in silicon) were compared for  $\tau_{outdiffusion}$  and for  $\tau_{IG}$ . At a wafer thickness of 100 microns for p- wafers, the time to outdiffuse is faster than the time to getter at oxygen precipitates sites. As the number of precipitates increase,  $\tau_{IG}$  decreases. As solar cell devices become thinner, getting by outdiffusion and oxygen precipitation can be optimized and outdiffusion will be the principle getter mechanism.

## 1.6 Future Work

For iron gettering experiments on p++ with epitaxial wafer samples, iron can be evaporated onto the backside of the silicon wafer, evacuated and sealed into a quartz ampule, and annealed at high temperatures to diffuse iron into the silicon. A layer of silicide often forms on the iron-side surface of the silicon. This can be removed chemically. The sample must then undergo preparation for Schottky contact evaporation: cleaning, metals removal and oxide removal. Once Schottky contacts have been evaporated, DLTS measurements on sample purity can be taken. EBIC can also be used to measure free carrier diffusion lengths. Annealing temperatures for iron diffusion into the sample, and precipitate density of the samples can be varied to measure gettering effectiveness.

Quantifying precipitates for purposes of gettering experiments requires very clean silicon samples, with specific etchants for specific boron doping concentrations in the

silicon wafers. In order to use EBIC and other spectroscopic equipment to determine precipitate density (other internal aspects of the silicon samples), good Schottky contacts must be evaporated onto the samples. Very high concentrations of oxygen precipitates make quantifying precipitate densities difficult. In order to form highly rectifying Schottky contacts, a clean, oxide free smooth surface on the silicon must be present.

All these findings are needed for iron gettering experiments. Precipitate densities are necessary to compare gettering effects of varying iron concentrations in the silicon, while good Schottky contacts are needed to run DLTS experiments on the samples.

## Appendix A: DLTS on p++ wafers

DLTS measurements were taken of the pure p++ samples from industry to test purity levels and to use as a control for future gettering experiments:

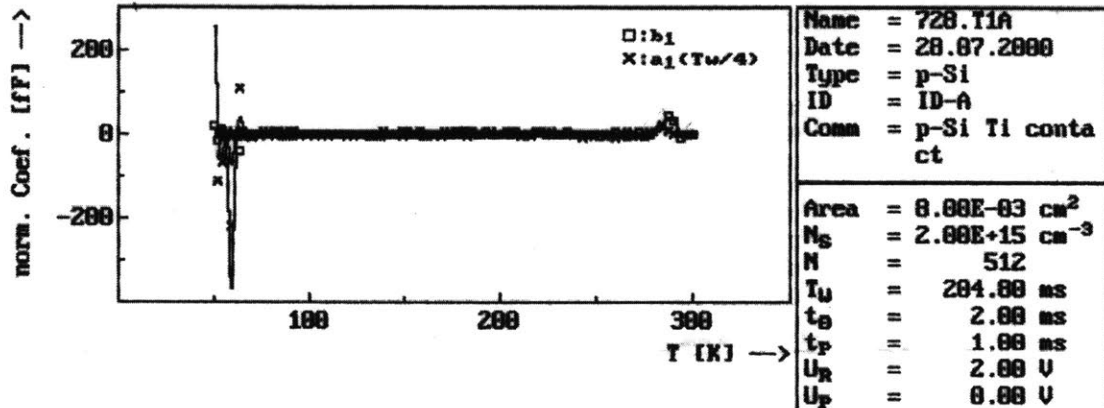


Figure 12: Normal Coefficient vs. Temperature for p++ wafers with DLTS

This graph represents the sample purity. Only one small deep level can be detected from any contamination. The wafer is very pure. The following Capacitance vs. Voltage curve is not perfectly linear, suggesting unevenness in doping. At high doping, current will not penetrate past a couple microns into the sample [12], so the following readings are for the epilayer region only:

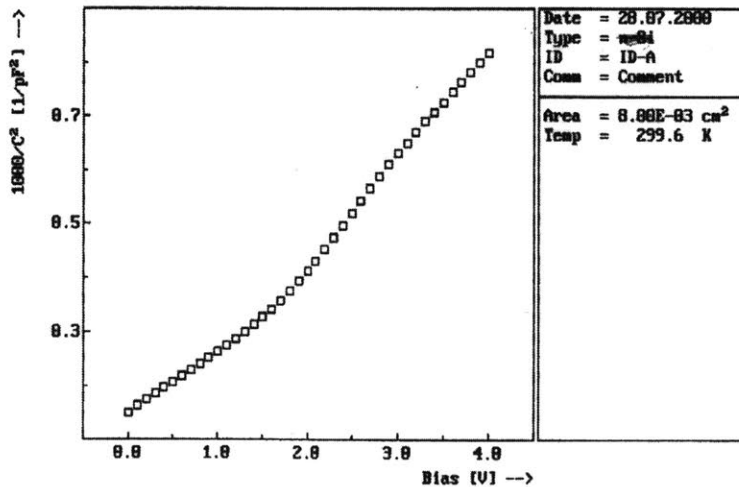


Figure 13: DLTS 1/C<sup>2</sup> Curve Versus Voltage of p++ Sample

## 1.8 References

- [1] Green, Martin A. *Solar Cells: Operating Principles, Technology, and System Applications Ch 2-Review of Semiconductor Properties*, University of New South Wales Publishing, 1992
- [2] Green, Martin A., *Solar Cells: Chapter 4-pn junction diodes*, University of New South Wales Publishing, 1992
- [3] Ahn, Sang Hoon, *Electrical Studies of Silicon and Low K Dielectric Material*, Massachusetts Institute of Technology, June, 1999
- [4] Smith, Aimee, Ahn S.H., Kimerling, L.C., *A Gettering Simulator: Polished Wafers and p/p++ Epilayers*, Electrochemical Society Proceedings Vol 98-1,
- [5] Tan T.Y., Taylor, W.J., *Mechanisms of Oxygen Precipitation: Some Quantitative Aspects*, Academic Press, 1994
- [6] Inoue, N., Wada, K., and Osaka J., *Semiconductor Silicon 1981*, The Electrochemical Society, Pennington, N.J., p 281
- [7] Burke, J., *The Kinetics of Phase Transformations in Metals*, Chapter 5, Pergamon Press, London, 1965
- [8] Livingston, F.M., Messoloras S., Newman R.C., Pike B., *Journal of Physics C: Solid State Physics*, Vol 17, 1984, p 6253
- [9] Isomae, Aoji, Watanabe, *Journal of Applied Physics*, Vol 55, 1984, p817
- [10] Schrems, M, *Proceedings of the 5<sup>th</sup> International Conference on Shallow Impurities in Semiconductors*, p231, Materials Science Forum, Vols 117-118, Switzerland, 1993
- [11] Schrems, M, *Simulation of Oxygen Precipitation in Czochralski Grown Silicon*, Materials Science and Engineering, B4 (1989) p393-399
- [12] Miller, Lang and Kimerling, *Capacitance Transient Spectroscopy*, Annual Review of Materials Science, 1977, 377-448